An EPR study of Cr^{3+} centres having monoclinic symmetry in $TlZnF_3$ single crystals

2008 J. Phys.: Condens. Matter 20 145202

(http://iopscience.iop.org/0953-8984/20/14/145202)

J. Phys.: Condens. Matter **20** (2008) 145202 (7pp) doi:10.1088/0953-8984/20/14/145202

An EPR study of Cr^{3+} centres having monoclinic symmetry in $TlZnF_3$ single crystals

H Ebisu[1], M Arakawa[2,4] and H Takeuchi[3]

[1] Department of Electrical and Computer Engineering, Nagoya Institute of Technology, Nagoya 466-8555, Japan
[2] Department of Materials Science and Engineering, Nagoya Institute of Technology, Nagoya 466-8555, Japan
[3] Department of Advanced Science and Technology, Toyota Technological Institute, Nagoya 468-8511, Japan

Received 3 December 2007, in final form 8 February 2008
Published 4 March 2008
Online at stacks.iop.org/JPhysCM/20/145202

Abstract

EPR measurements have been made on as-grown single crystals of $TlZnF_3$ doped with chromium. From Cr-only-doped crystals, two types of Cr^{3+} spectra with monoclinic symmetry were observed together with three kinds of Cr^{3+} spectra with trigonal symmetry which has been reported in our previous work (Ebisu *et al* 2005 *J. Phys.: Condens. Matter* **17** 4653–63). The obtained fine structure parameters for the monoclinic spectra are analysed using the spin-Hamiltonian separation method. Each monoclinic spectrum is ascribed to a Cr^{3+} ion, respectively, at a Zn^{2+} ion site in a ZnF_6 unit or a Zn_2F_9 unit with a Tl^+ vacancy. Distortions of the ligand octahedra are discussed using the separated axial parameters.

1. Introduction

The tolerance factor of $TlZnF_3$ ($t = 1.01$) is close to the boundary of those for the cubic perovskite crystals and the hexagonal $BaTiO_3$ type crystals [2, 3]. The real $TlZnF_3$ crystal has hexagonal $BaTiO_3$ type structure until 4.2 K with no structural phase transitions on lowering temperature from the melting point. The crystal structure is shown in figure 1. The structure has two types of Zn^{2+} ion sites. One Zn^{2+} site is in a ZnF_6 unit of a single octahedron (denoted by Zn_I). The fluorine octahedron is linked to other octahedra at the corner similarly to the octahedra in the cubic perovskite crystals. The other site is in a Zn_2F_9 unit composed of two face-sharing octahedra (denoted by Zn_{II}). In figure 1, three kinds of Tl^+ ions in the neighbourhood of the Zn^{2+} ions are shown by $Tl_{(1)}$, $Tl_{(2)}$ and $Tl_{(3)}$. In each TlF layer, the Tl^+ ions form a triangular sub-lattice. The a and a' denote the crystal axis directions in the c plane. For both Zn_I and Zn_{II} sites, the $a'c$ planes include some of the ligand fluorines and the Tl^+ ions but the ac planes do not.

The environment of the divalent cation may be considered to be an intermediate structure between that in a cubic perovskite crystal and that in a $CsNiCl_3$-like hexagonal crystal having the linear arrays of face-sharing octahedra [1, 4, 5]. It is interesting to investigate magnetic impurity centres formed in $TlZnF_3$ crystals in comparison with the formation of the magnetic impurity centres in perovskite and $CsNiCl_3$-like crystals. In the previous work [1], we reported the results of the electron paramagnetic resonance (EPR) experiments for the $TlZnF_3$ crystals doped with chromium, where for the Cr-only-doped as-grown crystal three kinds of Cr^{3+} centres with trigonal symmetry about the c axis are identified as the uncompensated Cr^{3+} centre at the Zn_I site (centre A), the uncompensated Cr^{3+} centre at the Zn_{II} site (centre B), and Cr^{3+}–V_{Zn} pair centre at the Zn_{II} sites (centre C). In some as-grown crystals, weak EPR spectra having low symmetry were observed. The authors carried out further EPR measurements for investigating the low-symmetric chromium centres in comparison with the above trigonal Cr^{3+} centres.

In this paper, we will report results of the EPR experiments for two types of low-symmetric chromium centres formed in $TlZnF_3$ crystals doped only with chromium. In section 3, the spin-Hamiltonian parameters will be determined from angular variations of these spectra. In section 4, the fine structure parameters obtained for the monoclinic Cr^{3+} centres in $TlZnF_3$

[4] Present address: Nakagawa-ku, Nagoya 454-0817, Japan.

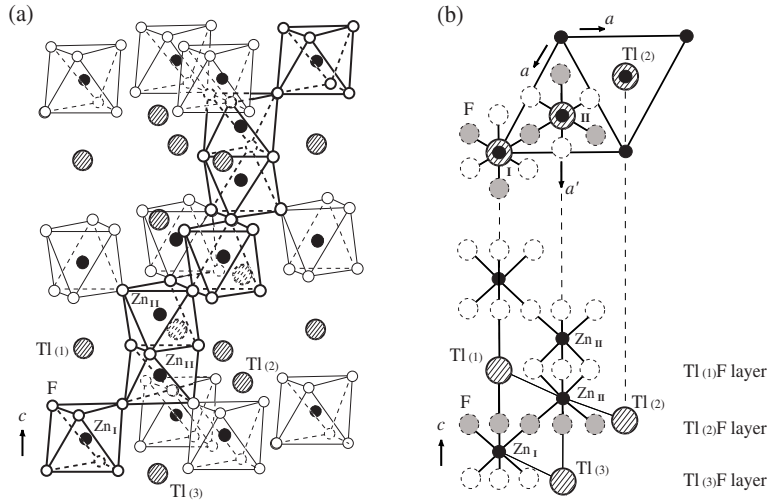

Figure 1. The hexagonal crystal structure of $TlZnF_3$. Small black circles denote Zn^{2+} ions. The marks Zn_I and Zn_{II} show the Zn^{2+} ions at the sites I and II, respectively. Open circles in (a) and medium size circles in (b) denote F^- ions. $Tl_{(1)}$, $Tl_{(2)}$ and $Tl_{(3)}$ denote the different types of Tl^+ ions relative to the Zn_I and Zn_{II} ions. The upper part of (b) shows the projection of the Zn^{2+} and the surrounding ions onto the *c* plane. Arrows *a* and *a*′ denote the crystal axis directions in the *c* plane. In the $Tl_{(1)}F$, $Tl_{(2)}F$ and $Tl_{(3)}F$ layer, the Tl^+ ions form triangular sub-lattices.

will be analysed using the spin-Hamiltonian separation method of the fine structure terms [5]. By discussing the separated axial parameters in comparison with the axial parameters for the trigonal Cr^{3+} centres, each monoclinic spectrum will be ascribed to a respective Cr^{3+} ion associated with a Tl^+ vacancy. The distortion of the ligand octahedron will be discussed using the separated axial parameters.

2. Experimental procedures

Single crystals of $TlZnF_3$ doped with chromium were grown by the Bridgman technique. Starting mixtures of TlF and ZnF_2 powders and a trace of CrF_3 powder (about 0.3 mol%) were sealed in glassy carbon crucibles. The crucibles were heated to 450 °C to yield liquid mixtures. Then, the temperature of the crucibles was lowered slowly with a cooling rate of about 50 °C h^{-1}. Obtained crystals had some natural planes of the hexagonal structure. EPR measurements were made at room temperature using a JES-FE1XG X-band spectrometer at the Instrument and Research Technology Center in Nagoya Institute of Technology. An NMR probe was used for accurate measurements of the external magnetic field.

3. Results

Figure 2 shows EPR spectra observed for a chromium-doped single crystal of $TlZnF_3$ at room temperature when the external magnetic field **H** is parallel to the crystalline *c* or *a* axes. The signals marked with A, B and C are the aforementioned trigonal Cr^{3+} centres [1]. Other weak signals marked with E and F in figure 2 come from some low-symmetric Cr^{3+} centres. We focus our attention on these low-symmetric centres in this work. Angular variations of the EPR spectra when the external field is rotated from the *c* to *a* axis are shown in figure 3. The open triangles and squares denote the angular variations of the experimental fields for signals E and F, respectively.

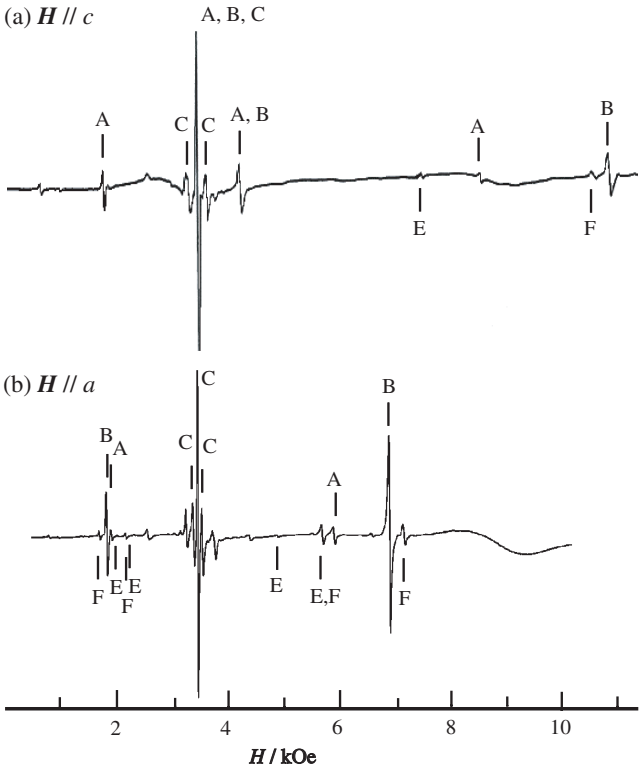

Figure 2. EPR spectra observed at 297 K from an as-grown crystal of $TlZnF_3$ doped with chromium when (a) **H** ∥ *c* and (b) **H** ∥ *a*. The signals marked with A, B, C, E and F correspond to different kinds of chromium centres.

In contrast to the trigonal centres A and B, both signals E and F with **H** ∥ *c* split into three branches with declined angles of the external field from the *c* axis. On the other hand, in the direction with **H** ∥ *a* for each centre, two branches coincide and the third branch shows an extremum at another field. These

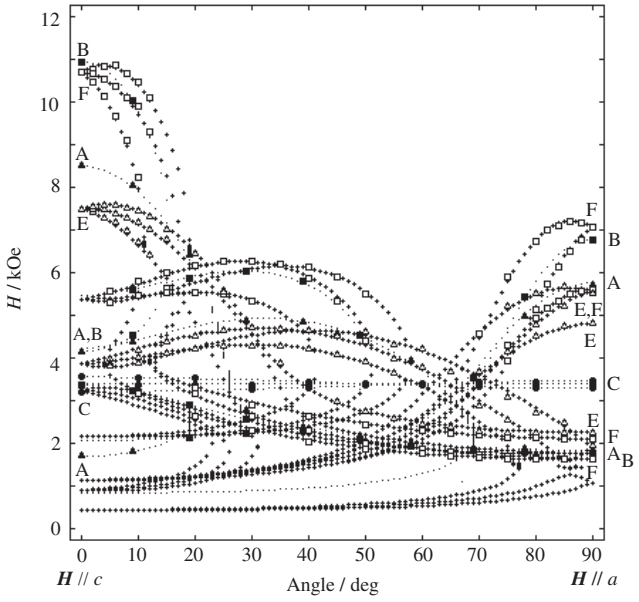

Figure 3. Angular variations of resonant fields of signals E and F. Open triangles and squares, and closed triangles, squares and circles, denote the angular variations of the experimental fields for signals E, F, A, B and C, respectively. The crosses indicate the theoretical fields for centres E and F and the dots for centres A, B and C, respectively.

features indicate that signals E and F are due to the Cr^{3+} centres associated with some defects (called centres E and F). As the branches of the EPR spectrum for centre F vary around the spectrum for centre B, centre F is considered to be a perturbed one for the uncompensated centre B at a Zn_{II} site.

Figure 4 shows a comparison of the angular variations for centre F in a high field region when the external field is rotated in the ac and $a'c$ planes. When the external field is rotated in the ac plane not including ligand F^- and Tl^+ ions, the high field signal at $\mathbf{H} \parallel a$ splits into two branches but the low field one does not split, as shown in figure 4(a). On the other hand, when the external field is rotated in the $a'c$ plane including some of the ligand F^- and Tl^+ ions, each signal at $\mathbf{H} \parallel a'$ splits into two branches having extrema with small angles to the a' axis as shown in figure 4(b).

Figure 5(a) shows the angular variations of the observed signals for centres E and F in the high field region with **H** in the c plane. Open triangles and squares denote the respective experimental fields of centres E and F. The closed triangles and squares having no angular variations denote the signals for the trigonal Cr^{3+} centres A and B. Both angular variations of centres E and F are composed of three branches, each of which shows an extremum separated by 60° from those of the other branches. The above feature of the spectra indicates that the main principal axes for centres E and F are declined from the crystalline c axis. In the directions with $\mathbf{H} \parallel a$ and $\mathbf{H} \parallel a'$, two branches coincide and the third branch shows an extremum at another field. It must be emphasized that both the angular variations of the branches marked with (2, 5) in figures 4(a) and 5(a) show the extrema in the a-axis direction, which is normal to the plane including the c axis and Tl^+ ions marked with (2, 5) or (2′, 5′) shown in figure 5(b).

The above features of the spectra indicate that centre F is a Cr^{3+} centre having a monoclinic symmetry with the main principal axis tilted from the crystalline c axis in the $a'c$ plane. There are six different tilting directions, which are separated from neighbouring directions by 60° when they are projected onto the c plane. Resonant fields of centre E show similar angular variations with a monoclinic symmetry to those of centre F. These facts suggest that the monoclinic centres E and F are formed by the perturbation for centres A and B due to Tl^+ vacancies in the $a'c$ planes respectively.

In the following section, we will analyse the fine structure terms for centres E and F using the spin-Hamiltonian separation method [5] to examine the above expectation in detail. Here, we only try to examine the consistency of the angular variation patterns with the assumption of Tl^+ ion vacancies as charge compensators. In figure 5(b), $Tl_{(1)}$ and $Tl_{(2)}$ sites are denoted by open and shaded circles respectively. If the Cr^{3+} ions at a Zn_{II} site are associated with the Tl^+ vacancies (V_{Tl}) of the $Tl_{(1)}$ type, six kinds of the Cr^{3+}–V_{Tl} pairs exist, as shown in figure 5(b) by the broken lines numbered from 1 to 6. In this case, the numbers attached to the EPR branches in figures 4 and 5(a) correspond to the numbers in figure 5(b). On the other hand, if the Cr^{3+} ions are associated with the Tl^+ vacancies of the $Tl_{(2)}$ type, six kinds

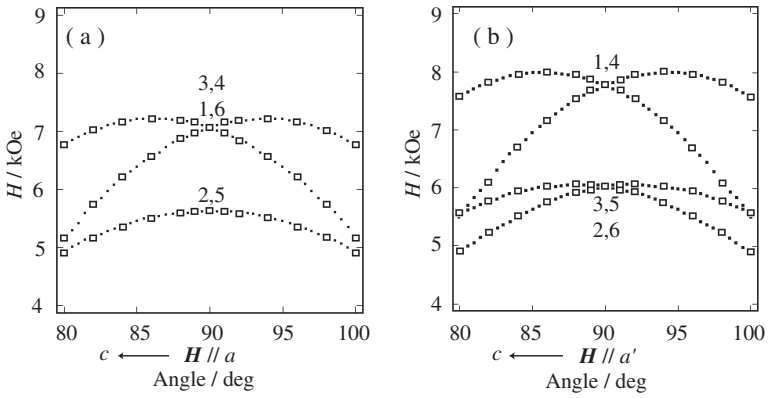

Figure 4. Angular variations of the signals for centre F observed at 297 K with **H** in the (a) ac and (b) $a'c$ planes. Open squares denote the experimental fields and dotted curves the theoretical fields.

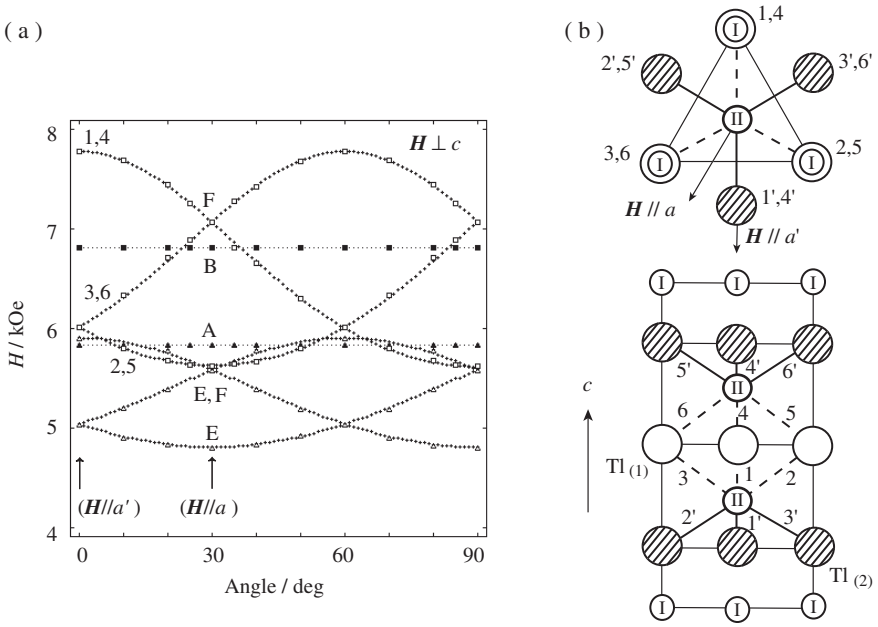

Figure 5. (a) Angular variations of the signals for centres E and F observed at 297 K with **H** in the c plane. Open triangles and squares denote the respective variations of the experimental fields for centres E and F. Dotted curves indicate the theoretical fields computed using the parameters given in table 1. (b) I and II in the small circles denote, respectively, the Zn_I and Zn_{II} sites. The large open and shaded circles show $Tl_{(1)}$ and $Tl_{(2)}$, respectively. The numbers with and without dashes denote the distinct types of Zn_{II}–$Tl_{(2)}$ pairs and Zn_{II}–$Tl_{(1)}$ pairs, respectively.

Table 1. Spin-Hamiltonian parameters obtained at 297 K for two kinds of monoclinic Cr^{3+} centres in $TlZnF_3$. Units are in 10^{-4} cm^{-1} for b_n^m.

Centre	g_x	g_y	g_z	b_2^0	b_2^2	α (deg)
E	1.9711(2)	1.9728(2)	1.9721(2)	−1954.1(2)	+541.6(2)	4.72(5)
F	1.9714(2)	1.9716(2)	1.9738(2)	+3462.4(2)	−1037.0(2)	4.15(5)

of the Cr^{3+}–V_{Tl} pairs also exist, as shown by the thick solid lines numbered from 1 to 6 with dashes. Each of $Cr^{3+}{}_{(II)}$–$V_{Tl(1)}$ and $Cr^{3+}_{(II)}$–$V_{Tl(2)}$ centres can give the branch pattern of the angular variations shown in figures 4 and 5(a). As the other possibility, if the Cr^{3+} ions at a Zn_I site are associated with the Tl^+ vacancies of the $Tl_{(3)}$ type, six kinds of the Cr^{3+}–V_{Tl} pairs also exist and the $Cr^{3+}_{(I)}$–$V_{Tl(3)}$ centre can give the above branch pattern of the angular variations.

We choose the principal z, x axes in the $a'c$ symmetry plane, where the z and x axes are declined from the c axis respectively by angles α and $\frac{\pi}{2} + \alpha$. This angle α corresponds to the angle of the extrema of the branches at about 8 kOe in figure 4(b) to the $\mathbf{H} \parallel a'$ direction. With this tilt angle α of the z axis, the term $\frac{1}{3}b_2^1 O_2^1$ vanishes in the spin Hamiltonian. Then, the spectra of centres E and F can be described within the experimental errors by the following spin Hamiltonian with $S = \frac{3}{2}$:

$$\mathcal{H} = g_x\beta S_x H_x + g_y\beta S_y H_y + g_z\beta S_z H_z + \tfrac{1}{3}(b_2^0 O_2^0 + b_2^2 O_2^2), \quad (1)$$

where O_2^0 and O_2^2 are the Stevens operators [6]. The spin-Hamiltonian parameters were fitted to the spectra by matrix diagonalization. Obtained values of the parameters are listed in table 1. For both centres, the fine structure parameters b_2^0 and b_2^2 are determined by the fitting to be of opposite signs. From the spectra, centres E and F are considered to be perturbed ones for centres A and B reported in the previous work [1]. So, the signs of b_2^0 for centres E and F listed in table 1 are assumed to be the same as those for the corresponding centres. In the following section, absolute signs of the b_2^0 parameters in the table will be shown to be reasonable by the spin-Hamiltonian separation analysis, and the tilt direction of the z axis from the c axis will be discussed in relation to the structures of the monoclinic centres.

4. Discussion

The spin-Hamiltonian separation method was first proposed to identify several low-symmetric Cr^{3+} centres [7] and later applied successfully to other Cr^{3+}, Fe^{3+} and Gd^{3+} centres with low symmetries. Here, we analyse the structure of centres E and F using this method.

The spectra of centres E and F have monoclinic symmetry with the zx symmetry plane. This suggests that the Cr^{3+} ions in centres E and F are perturbed by some charge compensators in the zx plane. As the uncompensated Cr^{3+} centres at the substitutional Zn_I and Zn_{II} sites have trigonal symmetry about the crystalline c axis, we try to separate the fine structure terms of the monoclinic centres E and F into the uniaxial terms along the c axis denoted by the z' direction and along a direction denoted by the z'' direction in the monoclinic symmetry plane

Table 2. Values of the separated parameters $b_{2a(1)}$, $b_{2a(2)}$ and ϕ at 297 K for the monoclinic Cr^{3+} centres E and F formed in $TlZnF_3$. Values for the trigonal centres A and B in $TlZnF_3$ and the monoclinic Cr^{3+} centre II and the trigonal Cr^{3+} centre I formed in $CsMgCl_3$ are also listed for comparison. Values in the last column are the ratios of $b_{2a(1)}$ to b_2^0 for the corresponding uncompensated trigonal centres. Units are in 10^{-4} cm^{-1} for the fine structure parameters.

Crystal	Centre	$b_{2a(1)}$	$b_{2a(2)}$	ϕ (deg)	ϕ–α (deg)	b_2^0 (trig)	Ratio
$TlZnF_3$	E	−1847.6	+435.1	+67.9	+63.2	—	0.774
	A[a]	—	—	—	—	−2387.0	—
	F	+3209.3	−783.9	+71.9	+67.7	—	0.918
	B[a]	—	—	—	—	+3496.9	—
$CsMgCl_3$	II[b]	+1397	−401	+75	+71	—	1.115
	I[b]	—	—	—	—	+1253.3	—

[a] After [1].
[b] After [5].

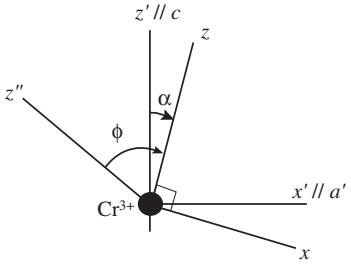

Figure 6. The principal axis (z, x axis) directions for the monoclinic centres E and F, and the uniaxial directions (z', z'' axes) in the spin-Hamiltonian separation analysis.

as follows:

$$\tfrac{1}{3}[b_2^0 O_2^0(z) + b_2^2 O_2^2(x, y)] = \tfrac{1}{3} b_{2a(1)} O_2^0(z') + \tfrac{1}{3} b_{2a(2)} O_2^0(z''), \tag{2}$$

where

$$O_2^0(z) = 3S_z^2 - S(S+1), \qquad O_2^2(x, y) = S_x^2 - S_y^2, \tag{3}$$

$$O_2^0(z') = 3S_{z'}^2 - S(S+1), \qquad O_2^0(z'') = 3S_{z''}^2 - S(S+1), \tag{4}$$

and $b_{2a(1)}$ and $b_{2a(2)}$ are the separated axial parameters. The relationships among the axis directions are shown in figure 6.

The main principal z axis is declined from the c axis by the angle α toward the x axis. The z'' axis is defined by an angle ϕ in figure 6. The separated parameter $b_{2a(1)}$ represents the axiality about the c axis corresponding to the axiality of the unperturbed centre. The other separated parameter $b_{2a(2)}$ represents the axiality caused by the perturbation. Equation (2) holds when the following conditions are satisfied [5]:

$$b_{2a(1)} \sin 2\alpha + b_{2a(2)} \sin 2\phi = 0, \tag{5}$$

$$b_{2a(1)} + b_{2a(2)} = b_2^0 + b_2^2, \tag{6}$$

$$\tan\phi = -\frac{2b_2^2}{(3b_2^0 + b_2^2)\tan\alpha}. \tag{7}$$

The separated axial parameters $b_{2a(1)}$, $b_{2a(2)}$ and the angle ϕ can be calculated by equations (5)–(7) from the experimental values of b_2^0, b_2^2 and α listed in table 1. The obtained values are tabulated in table 2, where the b_2^0 parameters for the related trigonal centres are also listed for comparison.

A monoclinic Cr^{3+} centre (centre II) is reported in another type of hexagonal crystal $CsMgCl_3$ [5], where excess positive charge on the substitutional Cr^{3+} ion is compensated by a nearest Cs^+ vacancy. In table 2, the axial parameters for the centre are listed for comparison. As seen from the table, each separated parameter $b_{2a(1)}$ for centres E and F in $TlZnF_3$ and for centre II in $CsMgCl_3$ is comparable with b_2^0(trig.) for the corresponding uncompensated centre in the same host crystal. This shows that the separation method can be successfully applied to the monoclinic centres and the absolute signs of b_2^0 and b_2^2 listed in table 1 are reasonable. Thus, the Cr^{3+} ions in centres E and F are considered to be at the Zn_I and Zn_{II} sites, respectively. At the same time, the result supports the conclusion in the previous work [1] that centre A is ascribed to an uncompensated Cr^{3+} ion at the ZnF_6 unit in spite of its large negative value of b_2^0. The other axial parameter $b_{2a(2)}$ is related to the associated charge compensator. The angle $\phi-\alpha$ is related to the direction of the nearest monovalent cation declined from the c axis. For centres E and F, the angles are close to that for centre II in $CsMgCl_3$ as shown in table 2. This shows an association with a monovalent Tl^+ vacancy for each centre E and F in spite of the small tilt angle α. It should be noted that the direction of the main principal z axis is declined by α in the opposite direction to the Tl^+ vacancy.

In each Cr^{3+}–V_{Tl} centre, the excess positive charge on the Cr^{3+} ion relative to the host Zn^{2+} ion is compensated locally by the Tl^+ vacancy. There are three types of possible Cr^{3+}–V_{Tl} centres as shown in figure 7, that is, the Cr^{3+} at a Zn_{II} site associated with a vacancy of $Tl_{(1)}$ (type 1), the Cr^{3+} at a Zn_{II} site associated with a vacancy of $Tl_{(2)}$ (type 2), and the Cr^{3+} at a Zn_I site associated with a vacancy of $Tl_{(3)}$ (type 3). From the above discussion, centre E may be identified to be a type-3 Cr^{3+}-V_{Tl} centre and centre F to be either a type-1 or type-2 Cr^{3+}–V_{Tl} centre.

Although the lattice parameters a are different among the isomorphous crystals $BaTiO_3$ (a = 5.735 Å) [8], $TlZnF_3$ (a = 5.934 Å) [9] and $CsMnF_3$ (a = 6.213 Å) [10], the ratio of the lattice parameters c/a(= 2.45) for $TlZnF_3$ is almost the same as 2.45 for $BaTiO_3$ and 2.43 for $CsMnF_3$. So, the differences of the environments among three types of Zn^{2+}–Tl^+ pairs in $TlZnF_3$ may be similar to the corresponding ones in $BaTiO_3$ and $CsMnF_3$. From the crystallographic data for

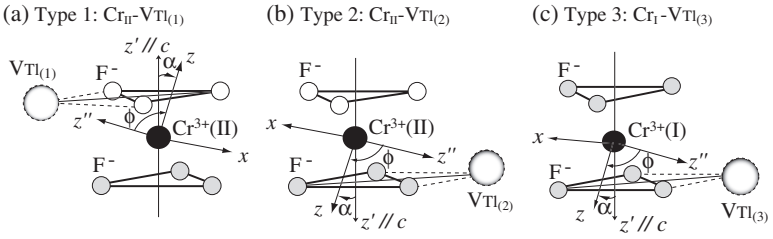

Figure 7. Three types of models for the monoclinic Cr^{3+} centres E and F in $TlZnF_3$.

$BaTiO_3$, we obtain the Ti–Ba distances and the angles of Ti–Ba directions with the c axis as follows: (3.54 Å, 69°) for type 1, (3.43 Å, 75°) for type 2, and (3.58 Å, 68°) for type 3. Although the distance is smallest for type 2, the angle 68° of centre F is closer to those for types 1 and 3. On the other hand, the cation–anion distances in the octahedra are as follows: 1.96 Å (site I) and 1.96 Å, 2.02 Å (site II) in $BaTiO_3$; and 2.098 Å (site I) and 2.113 Å, 2.164 Å (site II) in $CsMnF_3$. These data show that the space in the octahedron for the substitution of impurity ion is wider for site II than that for site I in both crystals.

For the trigonally symmetric Cr^{3+} centres, McGarvey [11, 12] suggested on the basis of his theoretical calculation that the sign of the b_2^0 parameter is related to the trigonal distortion of the ligand octahedron from the regular configuration. He considered that the distribution of the d electrons is concentrated more along the trigonal axis by a compression of the ligand octahedron along the axis. Later, Manoogian's group [13–16] examined by means of EPR and ENDOR experiments the relationship between the signs of b_2^0 and the distortions of the ligand octahedra for the trigonal Cr^{3+} centres formed in several single crystals. Their results indicated an empirical rule that negative (or positive) b_2^0 corresponds to the effective positive (or negative) surrounding charge distribution along the trigonal axis due to a compression (or elongation) of the octahedron along the trigonal axis. The positive values of $b_{2a(1)}$ for centre II and b_2^0 for centre I in $CsMgCl_3$ support the above empirical rule that the octahedra surrounding the Cr^{3+} ions in both centres are elongated along the crystalline c axis relative to the regular octahedral configuration. In the previous work [1], the large positive value of b_2^0 for centre B formed at the Zn_2F_9 unit was understood in terms of the elongation of the octahedron surrounding the Cr^{3+} ion due to the increased cation–cation repulsion between the Cr^{3+} and Zn^{2+} ions. The large positive value of $b_{2a(1)}$ for centre F suggests that the fluorine octahedron surrounding the Cr^{3+} ions is also elongated along the c axis, similarly to the case in centre B. On the other hand, the ligand octahedron in centre E may be compressed along the c axis, as $b_{2a(1)}$ for centre E is negative.

It must be emphasized that the separated axial parameter $b_{2a(2)}$ for centre E has a different sign from that for centre F, although the separated parameters for both centres are related to the respective Tl^+ vacancies. Here, we will examine the configuration of ligand octahedra using the knowledge of the axial parameters $b_{2a(2)}$ for centres E and F.

Figure 8 shows a distortion of the ligand octahedron by a Tl^+ vacancy, which is similar to the case of the K^+-vacancy-associated centres in the perovskite crystals [7, 17, 18]. Due

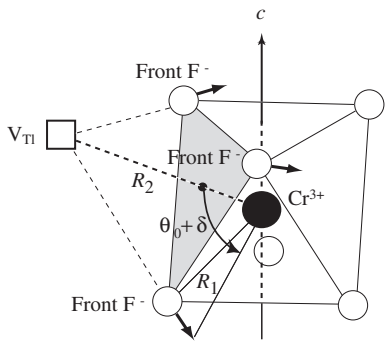

Figure 8. The front ligand deviations surrounding the Cr^{3+} ion by the presence of a monovalent cation vacancy V_{Tl}. R_1 and R_2 are the distances of the front F^- ion and V_{Tl} from the Cr^{3+} ion, $\theta_0 = \cos^{-1}\frac{1}{\sqrt{3}}$, and δ is the deviation angle of the front F^- ions from the regular octahedral configuration.

to the effective negative charge on the Tl^+ vacancy, the front F^- ions may be displaced away from the vacancy. By the perturbation calculation in the $^4F(3d^3)$ term within the framework of the point charge model, we obtain the following expression of the axial parameter $b_2^0(^4F)$ for the configuration shown in figure 8:

$$b_2^0(^4\mathrm{F}) = \frac{2\sqrt{2}}{7}\cdot\frac{\zeta^2 e^2}{\Delta^2}\left[\frac{1}{3\sqrt{2}}\left(\frac{\langle r^2\rangle}{R_2^3}+\frac{20}{27}\cdot\frac{\langle r^4\rangle}{R_2^5}\right)-\left(\frac{\langle r^2\rangle}{R_1^3}-\frac{5}{9}\cdot\frac{\langle r^4\rangle}{R_1^5}\right)\delta\right], \tag{8}$$

where $e = 4.80\times10^{-10}$ e.s.u., $\zeta = 273$ cm^{-1} [19], $\langle r^2\rangle = 1.45$ a.u. and $\langle r^4\rangle = 4.35$ a.u. [20]. The monovalent ion vacancy makes a positive contribution to $b_2^0(^4F)$ and three deviated front ligands with the deviation angle δ from the regular octahedral angle $\theta_0 = \cos^{-1}\frac{1}{\sqrt{3}}$ a negative contribution to $b_2^0(^4F)$. If we estimate roughly $R_1 = R_2/\sqrt{3} \simeq 2.02$ Å and $\Delta \simeq 15\,000$ cm^{-1} for fluorides (for example $\Delta = 16\,100$ cm^{-1} for Cr^{3+} in K_2NaCrF_6 [21]), the above two contributions cancel out when δ is about 3°. Thus, the positive sign of the axial parameter $b_{2a(2)}$ for centre E may be mainly due to the effective negative charge on the Tl^+ vacancy over the effect of the small front F^- deviations. This suggests that the F^- deviations by the Tl^+ vacancy may be rather difficult for the fluorines in the $Tl_{(2)}F$ and $Tl_{(3)}F$ layers in the type-3 model for centre E. In contrast, the negative sign of $b_{2a(2)}$ for centre F suggests that the

effective positive charge along the Cr^{3+}-V_{Tl} pair direction may arise due to the greatly compressed octahedra along the pair direction. So, front F^- deviations within the $Tl_{(1)}F$ layer may be easy compared with those within the $Tl_{(2)}F$ and $Tl_{(3)}F$ layers. As the type-1 and type-2 models for centre F include respectively two and one front F^- ions in the $Tl_{(1)}F$ layer, the octahedron in the type-1 model can distort more easily by the Tl^+ vacancy than that in the type-2 model. So, the type-1 model may be more feasible than the type-2 model for centre F.

5. Conclusions

From the Cr-only doped crystal of $TlZnF_3$, two Cr^{3+} centres with monoclinic symmetry (centres E and F) were observed in addition to the three kinds of Cr^{3+} centres with trigonal symmetry about the c axis (centres A, B, C). By the analysis using the spin-Hamiltonian separation method, the monoclinic centres were identified to be the Cr^{3+} centres formed at a ZnF_6 unit (Zn_I site) and a Zn_2F_9 unit (Zn_{II} site) associated with Tl^+ vacancies. Considering the values of the separated axial parameters $b_{2a(1)}$ and $b_{2a(2)}$, centre E is ascribed to a Cr^{3+} ion at a Zn_I site associated with a $Tl_{(3)}$ vacancy, and centre F is ascribed to a Cr^{3+} ion at a Zn_{II} site associated with a $Tl_{(1)}$ or $Tl_{(2)}$ vacancy. By the signs of the separated parameters $b_{2a(1)}$ and $b_{2a(2)}$, the ligand octahedron in centre E is considered to be compressed along the c axis and only weakly distorted along the Cr^{3+}–V_{Tl} bond axis, and the ligand octahedron in centre F is considered to be elongated along the c axis and compressed along the Cr^{3+}–V_{Tl} bond axis.

References

[1] Ebisu H, Arakawa M and Takeuchi H 2005 *J. Phys.: Condens. Matter* **17** 4653–63
[2] Babel D 1967 *Struct. Bond.* **3** 1–87
[3] Babel D 1969 *Z. Anorg. Chem.* **369** 117–30
[4] McPherson G L and Devaney K O 1980 *J. Phys. C: Solid State Phys.* **13** 1735–43
[5] Takeuchi H, Tanaka H and Arakawa M 1993 *J. Phys.: Condens. Matter* **5** 9205–14
[6] Abragam A and Bleaney B 1970 *Electron Paramagnetic Resonance of Transition Ions* (Oxford: Clarendon)
[7] Takeuchi H, Arakawa M, Aoki H, Yosida T and Horai K 1982 *J. Phys. Soc. Japan* **51** 3166–72
[8] Burbank R D and Evans H T Jr 1948 *Acta Crystallogr.* **1** 330–6
[9] Vollmer G 1966 *Dissertation* Tübingen
[10] Zalkin A, Lee K and Templeton D H 1962 *J. Chem. Phys.* **37** 697–9
[11] McGarvey B R 1964 *J. Chem. Phys.* **40** 809–12
[12] McGarvey B R 1964 *J. Chem. Phys.* **41** 3743–58
[13] Danilov A G and Manoogian A 1972 *Phys. Rev.* B **6** 4097–103
[14] Danilov A G and Manoogian A 1972 *Phys. Rev.* B **6** 4103–11
[15] Danilov A G, Vial J C and Manoogian A 1973 *Phys. Rev.* B **8** 3124–33
[16] Manoogian A and Leclerc A 1974 *Phys. Rev.* B **10** 1052–8
[17] Patel J L, Davies J J, Cavenett B C, Takeuchi H and Horai K 1976 *J. Phys. C: Solid State Phys.* **9** 129–38
[18] Krebs J J and Jeck R K 1972 *Phys. Rev.* B **5** 3499–505
[19] Griffith J S 1961 *The Theory of Transition-Metal Ions* (Cambridge: Cambridge University Press)
[20] Freeman A J and Watson R E 1965 *Magnetism* vol 2A, ed G Rado and H Suhl (New York: Academic)
[21] Ferguson J, Guggenheim H J and Wood D L 1971 *J. Chem. Phys.* **54** 504–7